Rare Metal Materials and Engineering
Volume 51, Issue 6, June 2022
Available online at www.rmme.ac.cn

Science Press

Cite this article as: Yang Jing, Zhang Yi, Dong Nan, et al. Segregation Behavior of Alloying Elements at NbC/fcc-Fe Interface and Effects of Boron[J]. Rare Metal Materials and Engineering, 2022, 51(06): 2056-2062.

ARTICLE

Segregation Behavior of Alloying Elements at NbC/fcc-Fe Interface and Effects of Boron

Yang Jing[1], Zhang Yi[1], Dong Nan[1], Li Huabing[2], Han Peide[1], Jiang Zhouhua[2]

[1] College of Material Science and Engineering, Taiyuan University of Technology, Taiyuan 030024, China; [2] School of Metallurgy, Northeastern University, Shenyang 110004, China

Abstract: Based on the first-principles method of density functional theory (DFT), the segregation behavior of Si, Ni, Mn, Cr, and Mo at the NbC/fcc-Fe interface was studied, and the influence of B on the segregation behavior of alloying elements was analyzed. The results show that Cr and Mo can stably exist in the interface and NbC. Mo tends to segregate in the interface and NbC; Ni and Mn have a slight tendency to interface segregation. Mo is easy to segregate into NbC to form composite carbides. When the Mo/Nb content ratio is less than 2/3, the (Nb, Mo)C composite carbide is more stable and the binding energy is greater, which should be related to the strong electronic interaction between Mo and C and between Mo and Fe. When B is doped to the interface, the tendency of Mo and Cr to segregate to the interface is suppressed, expecially the segregation of Mo at the interface, thereby improving the corrosion resistance of the material. In addition, B can make Ni and Mn tend to be uniformly distributed in the matrix.

Key words: alloying elements; segregation energy; NbC/fcc-Fe interface; boron; first principles

Compared with ordinary austenitic stainless steel, super austenitic stainless steel contains higher content of Cr, Ni, Mo, N and other elements, and has excellent resistance to uniform corrosion, pitting corrosion and other local corrosion and stress corrosion. It is widely used in flue gas desulfurization, waste incineration, desalination and petrochemical industries[1-4]. With the deterioration of the service environment, new requirements are put forward for the strength, corrosion resistance and heat resistance of the material. For high-molybdenum super austenitic stainless steel with Mo content of 6%~7%, in some cases, it can be comparable to iron-nickel-based alloys (such as C276 and titanium alloys) with excellent corrosion resistance, and its strength is mainly due to solid solution strengthening, but the improvement is limited[5]. Precipitation strengthening is the most effective strengthening method. The yield strength and tensile strength of stainless steel are significantly improved through the dispersed precipitates. The pin dislocations and grain boundaries of fine precipitates can inhibit the growth of grains during heat treatment. Grain refinement can effectively improve the strength and toughness of steel[6,7].

Nb and Ti are strong carbide forming elements. The austenitic stainless steel contains Ti, Nb and C which combine together to form fine and dispersed *MX* precipitates (NbC, TiC) to form lattice defects such as pin dislocations, and have a good strengthening and toughening effect. Niobium and molybdenum compounds have been added to microalloyed steel to realize the complementary advantages of the elements[8,9]. Several reviews have found that the carbides in Nb-Mo microalloyed steel are more dispersed and finer than those in Nb-Ti microalloyed steel. Zhou et al[10] found that there is a σ phase around NbC in 304H. They also used EDS and HR-FEM technology to analyze the distribution of Cr atoms in the NbC phase interface of austenitic stainless steel. There is an enrichment of chromium at the interface, which may be the early stage of the formation of σ phase. Some scholars[11] reported the addition of niobium in super austenitic stainless steel. Nb can improve the corrosion resistance of super austenitic stainless steel. However, whether there is a correlation between NbC and σ phase has seldom been reported yet. At present, many experimental and theoretical studies have been carried out on the characteristics of NbC precipitates and the NbC/bcc-Fe and NbC/fcc-Fe interfaces by adding Nb to stainless steel[12,13]. However, there are few

---

Received date: June 25, 2021
Foundation item: National Natural Science Foundation of China (U1860204, 51871159); Natural Science Foundation of Shanxi Province (201801D221125)

Corresponding author: Han Peide, Ph. D., Professor, Taiyuan University of Technology, Taiyuan 030024, P. R. China, E-mail: hanpeide@tyut.edu.cn

studies on the segregation behavior of alloying elements, especially Mo, at the NbC/fcc-Fe interface. Mo is an element that is easy to segregate and to form σ phase. If it precipitates at the NbC/fcc-Fe interface, it is unfavorable for super austenitic stainless steel [14,15]. This study used first principles to investigate the segregation behavior of alloying elements at the NbC/Fe interface and the effect of B on the segregation behavior of alloying elements.

1 Calculation Method and Model

1.1 Calculation method

All calculations in this study were performed using Vienna Ab initio Simulation Package (VASP) [16,17]. Perdew-Burke-Ernz-erhof (PBE) [18] exchange-correlation functional generalized gradient approximation (GGA)[19] at the semi-local DFT level was used together with the projector augmented wave (PAW) [20,21] method. The maximum plane wave truncation energy was 400 eV, and the K point was set to 8×8×1[22]. The force convergence threshold of self-consistent field iteration was set to 10^{-5} eV, the force acting on each atom was no more than 0.3 eV/nm, and the internal stress was no more than 0.05 GPa. There is a Baker-Nutting orientation relationship between niobium carbide and face-centered cubic iron[13], so the NbC(001)/fcc-Fe(001) interface model was built in this study, and its mismatch was 6.9%, and the interface mismatch can be expanded to 10% for the heterojunction interface[1]. The magnetic contributions were neglected and we restricted our calculations to the nonmagnetic state because the model of Fe in our manuscript was considered as fcc structure. The NbC interface of different layers and terminals were discussed, and 5 layers of NbC and 9 layers of fcc-Fe were selected finally.

1.2 NbC/fcc-Fe interface structure model

Based on the structure of NbC and fcc-Fe, an atomic structure model of the NbC/Fe interface with 5 Nb atoms, 5 C atoms and 18 Fe atoms (28 atoms in total) was established (Fig. 1a), where Fig. 1b shows the addition of B atoms at the NbC/Fe interface. The thickness of the vacuum layer was set to be 1 nm to avoid the interaction between adjacent interfaces caused by periodic boundary conditions. The lattice parameters of the interface structure system are $a=b=0.332\ 27$ nm, $c=3.578\ 74$ nm, and $\alpha=\beta=\gamma=90°$. The positions numbered from 1 to 5 in Fig. 1 are the replacement positions of the replacement atoms in the calculation, i. e. the replacement atom M= (Si, Ni, Mn, Cr, Mo). In order to ensure the conservation of the number of atoms in the interface model, when the replacement atom is at position 1 and 2 (replacement of Fe), position 3 is Fe atom; when the replacement atom is at position 4 and 5 (replacement of Nb), position 3 is Nb. When the replacement atom is in position 3, the remaining atoms remain unchanged.

The formation energy of the interface structure system can be determined by the following formula[23-25]:

$$H_f = \{ E_{tot}(\mathrm{NbC/Fe}) - m \cdot E(\mathrm{Fe}) - n \cdot E(\mathrm{Nb}) - k \cdot E(\mathrm{C}) - l \cdot E(\mathrm{M}) \} / (m + n + k + l) \tag{1}$$

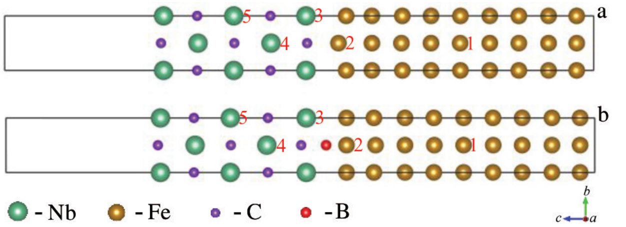

Fig.1 Calculation models: (a) NbC(001)/fcc-Fe(001) interface model, (b) interface structure after doping B at the interface (1, 2, 3, 4 and 5 are doping sites of alloying element M)

where E_{tot} (NbC/Fe) refers to the total energy of the NbC/Fe interface structure; m, n, k and l correspond to the number of Fe atoms, Nb atoms, C atoms and M alloy atoms in the structure, respectively; E(Fe), E(Nb), E(C) and E(M) are the total energy of each Fe atom, Nb atom, C atom and M alloy atom in the most stable elementary state, respectively.

The segregation energy (E_{Seg}) is used to express the tendency of the replacement atom M to segregate from the matrix to the phase interface. The segregation energy (E_{Seg}) can be determined by the following formula[26]:

$$E_{Seg} = E_{Interface}(\mathrm{NbC/Fe}) - E_{Bulk}(\mathrm{NbC/Fe}) \tag{2}$$

Among them, $E_{Interface}$ and E_{Bulk} are the total energy of the interface model where the replacement atom M occupies the interface area and the matrix area, respectively.

Griffith work of fracture, often called separation work, is used to evaluate the bonding ability (breaking strength) of the interface[27-29]. It is used to predict the cohesion or cohesion trend by adding replacement atom M. It refers to the energy required to separate the phase interface into two free surfaces or to break the phase interface.

$$W_{Frac} = [E_{(001)}(\mathrm{NbC}) + E_{(001)}(\mathrm{Fe}) - E_{Interface}(\mathrm{NbC/Fe})] / S \tag{3}$$

Among them, $S=ab$ is the cross-sectional area of the atomic layer at the interface, a and b are the lattice constants of the interface supercell, and $E_{(001)}$(NbC) and $E_{(001)}$(Fe) are the total energy of the free surface model.

2 Results and Discussion

2.1 Segregation tendency of alloying element at the interface

According to Eq. (1) and Eq. (2), the total energy of the interface structure after the replacement of atoms M (Si, Ni, Mn, Cr, Mo) at position 2~5 in the NbC/fcc-Fe interface structure system is recorded $E_{Interface}$; the total energy of the interface after the replacement of atoms M (Si, Ni, Mn, Cr, Mo) at the fcc-Fe (position 1) atom is set to E_{Bulk}. Fig. 2a and 2b show the formation energy and segregation energy of the system after the atom M replaced corresponding atoms at different positions at interface. As shown in Fig. 2a, the formation energies of alloy and unalloyed NbC/fcc-Fe interface structure system are all positive and close to zero, indicating that they are more difficult to form. Compared with the NbC/fcc-Fe interface system without alloying element replacement, Mo replacement is more conducive to the

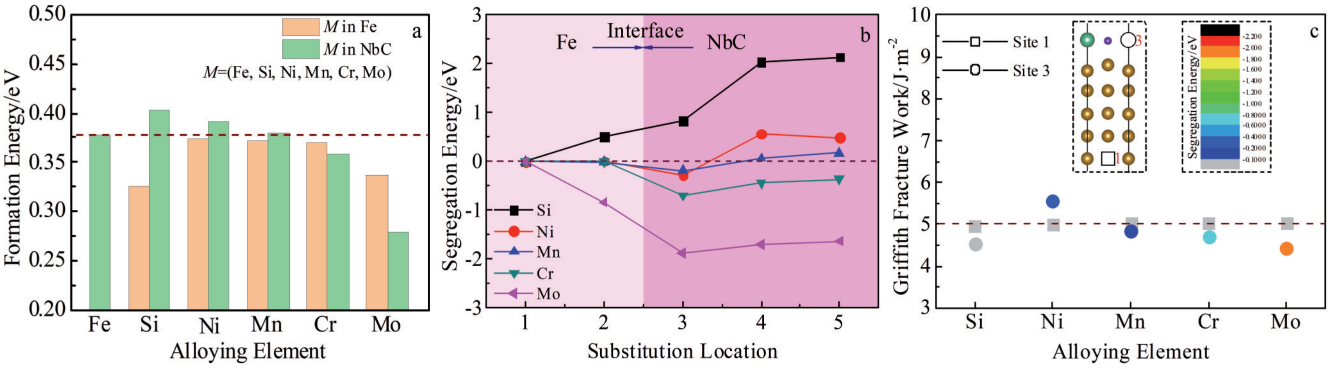

Fig.2 Formation energy of the system when the alloy elements are located at different positions (position 1/5) (a); segregation energy of the system when the alloy element are located at different positions (position 2/3/4/5) (b); Griffith fracture work of alloy interface (position 1/3) (c)

formation of Mo-containing interface system. Formation energy is the energy released or absorbed by different types of atoms from their elementary state to form compounds. Formation energy is used as a criterion for compound stability. The smaller the formation energy, the easier the dopant atoms to enter, that is, the more stable the interface. Judging from the formation energy of the NbC/fcc-Fe interface and the doped interface, Si, Ni, Mn can be stably doped in Fe, and Cr and Mo elements can be stably doped in Fe and NbC. As shown in Fig. 2b, Mo can stably exist in NbC with lower formation energy. The segregation tendency towards replacement atoms at the interface can be divided into three types. The first category: the E_{Seg} value of the replacement atom is positive, that is, this type of atom is stable in the Fe matrix, such as Si. The second category: the E_{Seg} value of the replacement atom (position 3) is negative, and E_{Seg} value of the remaining positions are almost positive. Results indicate that the replacement atom is slightly segregated at the interface, but there is no tendency to segregate into carbides, such as Mn and Ni. The third category: the E_{Seg} values are all negative, suggesting that the replacement atom is segregated at the interface, and there is a tendency to further segregate into carbides, such as Cr and Mo.

Fig. 2c displays the Griffith fracture work of the system after the replacement atoms are located at position 1 and 3, that is, the interface separation work after Si, Ni, Mn, Cr, Mo, etc are added in the matrix (position 1) and interface (position 3). The figure uses the segregation of the corresponding alloy elements to color these 5 kinds of replacement atoms. It can be seen that when the replacement atom is in the Fe matrix, it has no effect on the interface separation work (about 5 J/m^2). When the replacement atom is located on the NbC side of the interface, except for Ni, the interface separation work is generally lower than that of the replacement atom on the Fe matrix. The results indicate that when the replacement atom is at the interface, the binding capacity of the interface decreases. Combined with the segregation energy in Fig.2b, it can be seen that Si, Mn, and Ni atoms tend to be evenly distributed in the matrix, which has little effect on the binding ability of the NbC/fcc-Fe interface structure system. In addition, Cr and Mo atoms are more likely to be distributed in the NbC side of the interface, which is not conducive to the improvement of the binding ability of the NbC/fcc-Fe interface structure system. The most important role of Cr and Mo atoms in stainless steel is to improve the corrosion resistance of the material, that is, it is easier to play a role when dissolved in the matrix phase. Recently, after adding a small amount of boron to high austenitic stainless steel (S31254), it has the effect of suppressing the precipitation phase, that is, B can suppress the segregation of Cr and Mo to the austenite grain boundary. And whether B has an effect on the segregation of Mo and Cr to the NbC/fcc-Fe interface structure system has seldom been seen in the related studies, but the results are very important, so the following analysis will be carried out on the basis of the interface structure model.

2.2 Niobium-molybdenum composite carbide

The above analysis shows that Mo is most likely to segregate on the NbC side of the NbC/fcc-Fe interface structure system. B has a tendency to suppress the segregation of Mo to NbC at the NbC/fcc-Fe interface. In order to analyze the stability and electronic properties of the (Nb, Mo)C composite carbide formed by dissolving Mo in NbC, the following studies were conducted on the (Nb,Mo)C composite carbide. Fig. 3 shows the $(Nb_{0.8}M_{0.2})C$, $(Nb_{0.6}M_{0.4})C$, $(Nb_{0.4}M_{0.6})C$, $(Nb_{0.2}M_{0.8})C$ and MoC structure models constructed by dissolving different amounts of Mo in NbC. At the same time, the influence of Mo occupancy is considered.

Fig. 4 shows the formation energy and separation work of the interface structure system composed of (Nb, Mo)C composite carbide and Fe. Fig.4a shows the formation energy of the system. The increase in Mo content has a greater impact on the formation energy, that is, the higher the Mo content of (Nb, Mo)C, the higher the formation energy, and the more difficult it is to form, indicating that (Nb,Mo)C with high Mo content is difficult to form. The structure of the lowest total score is selected for Griffith fracture work calculation. Fig.4b shows that when the Mo/Nb content ratio reaches 1/4~2/3, the separation work is higher, that is, the binding ability is

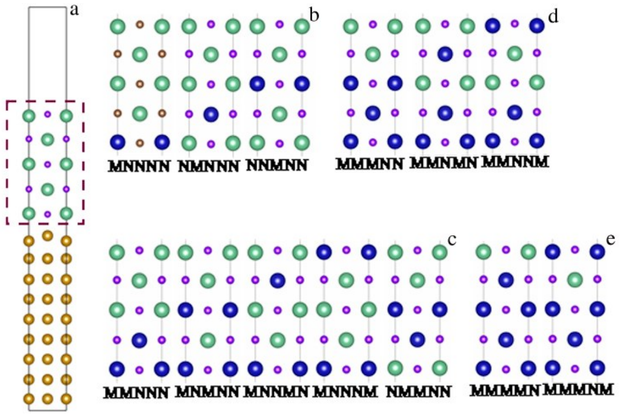

Fig.3 Supercell structures of NbC/Fe consisting of 18 Fe atoms, 5 Nb atoms, and 5 C atoms (a), $(Nb_{0.8}M_{0.2})C$ (b), $(Nb_{0.6}M_{0.4})C$ (c), $(Nb_{0.4}M_{0.6})C$ (d), and $(Nb_{0.8}M_{0.2})C$ (e) (green, gold, purple and bule balls are Nb, Fe, C and alloying atoms (Mo), respectively)

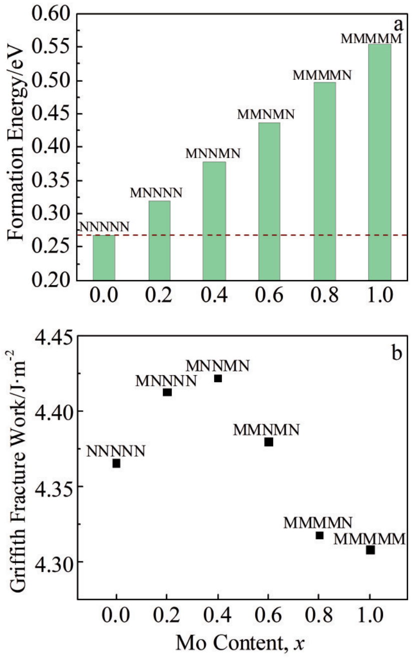

Fig.4 Formation energy (a) and Griffith fracture work (b) of $(Nb_{1-x}Mo_x)C/Fe$ with various Mo site fractions

stronger. When the Mo/Nb content ratio reaches 2/3, the interfacial bonding ability decreases. It can be concluded that the (Nb,Mo)C bonding ability formed by dissolving too much Mo in NbC is not good, which is not conducive to the improvement of toughness.

In order to further understand the role of Mo in the (Nb,Mo)C/Fe interface structure system, the projected density of states (PDOS) of the interface structure system was calculated. Fig.5a~5f show the d-orbital electrons of Nb(Mo), Fe1, Fe2 and the 2p-orbital electrons of the C atom at the (Nb, Mo)C/Fe interface. In the NNNNN/fcc-Fe interface structure of Fig. 5a, there are obvious hybridization peaks between Nb and C at −4.3, −4.1, and −3.8 eV, and there are also hybrid peaks of Nb, C and Fe at −3.8 eV. As Mo replaces Nb atoms, the number of hybrid peaks of Mo and C increases significantly, and the number of hybrid peaks of Mo and C and Fe also increases. Analyzing the TDOS value of the Fermi level, we found that it is approximately 43.96, 42.01, 36.32, 42.55, 46.26 and 45.92 (state/eV). The higher the TDOS value of the Fermi level, the stronger the metallicity of the system, and on the contrary, the stronger the covalentness of the system.

2.3 Effect of B on the tendency of interface segregation of alloy elements

Experimental studies have shown that the solubility of B in Fe is very low[30,31], so B is usually located at the grain boundary and plays a role of purifying the grain boundary. For this reason, this part first theoretically analyzes the occupancy trende of B at the NbC/fcc-Fe interface. The results show that the system energy of B in the Fe matrix is −247.47 eV, and the system energy of B at the interface is −249.87 eV. The calculated segregation energy of B at the interface is −2.40 eV, that is, B is easy to segregate at the interface, which is consistent with the experimental results. Therefore, the B atom is placed at the interface (as shown in the red ball in Fig.1b), and the tendency towards the replacement atom M (M =Si, Ni, Mn, Cr and Mo) to segregate at the interface was studied.

Also according to Eq.(1) and Eq.(2), the total energy of the system after the replacement of atoms M (Si, Ni, Mn, Cr, Mo) at position 2~5 of the NbC/fcc-Fe interface structure system containing B is recorded as $E_{\mathrm{Interface}}$; the total energy of the system after the replacement of atoms M (Si, Ni, Mn, Cr, Mo) at the fcc-Fe (position 1) of the NbC/fcc-Fe interface structure system containing B is set as E_{Bulk}. The formation energy and segregation energy of the system, i.e., the replacement atoms at different positions on the interface, were calculated, as shown in Fig.6a and 6b.

It can be seen from Fig.6a that compared to the unalloyed interface structure containing B at the interface, formation energy of the system is slightly reduced after Fe matrix is doped with Si, Ni, Mn, and Cr. After Mo is doped on the NbC side, its formation energy is lower. Similarly, the system in which the replacement atom is at a position of low formation energy corresponds to low segregation energy, that is, it is easy to form at this position. Comparing Fig.2a and Fig.6a, it can be concluded that the formation energy value of the interface structure system containing B at the interface is smaller, so it is easy to form. Fig.6b shows that the presence of B at the interface makes the segregation tendency towards Si, Ni, Mn, Cr, and Mo at the NbC/fcc-Fe interface weaker than that at the interface structure system without B, especially the greatest impact on Cr and Mo. First of all, for Cr, B prevents the segregation of Cr on the Fe matrix side and the NbC side of the interface, and also reduces its segregation tendency in NbC, which is more conducive to the uniform distribution of Cr in the matrix. For Mo, B can suppress the

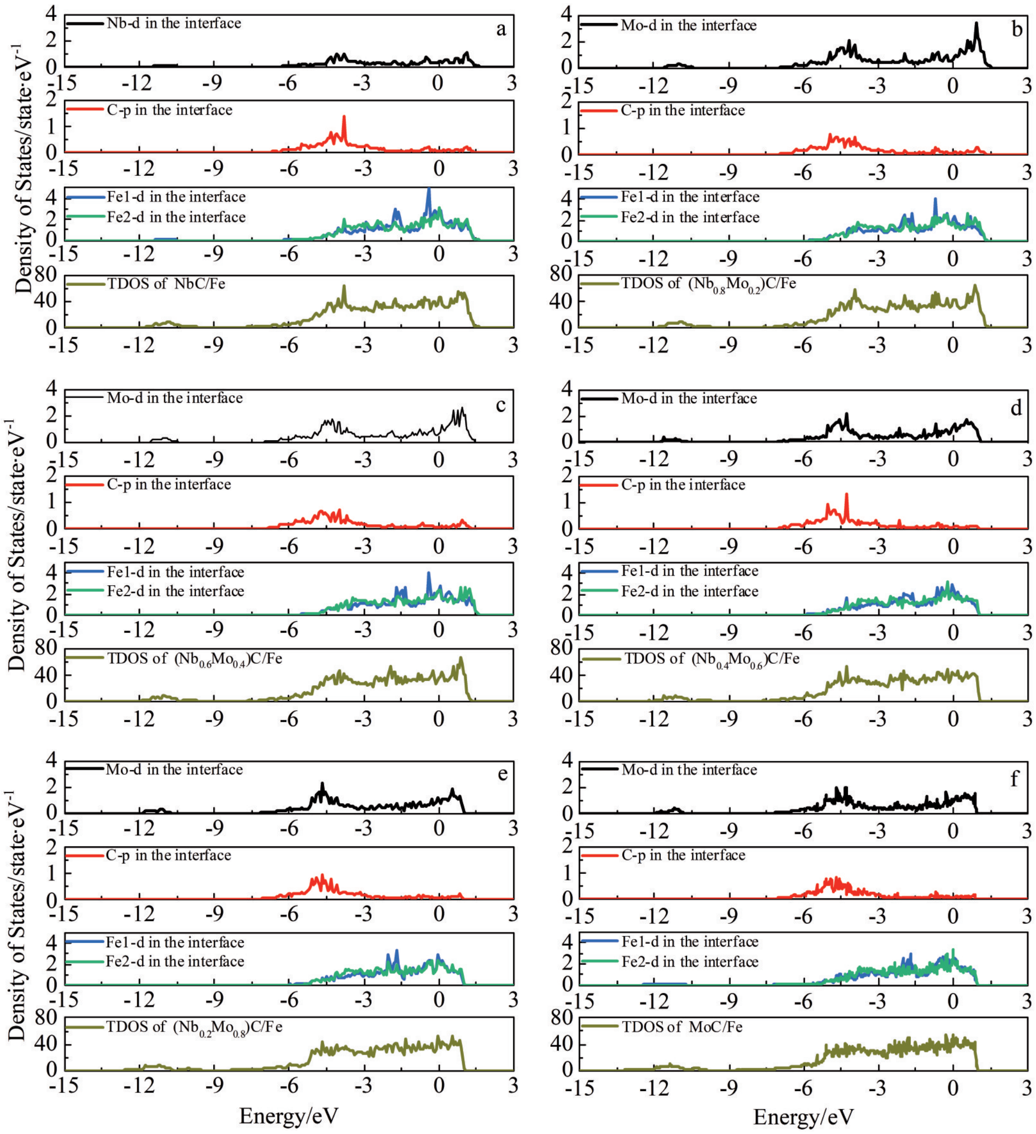

Fig.5 Projected density of states (PDOS) and total density of states (TDOS) of atoms at the interfaces of NNNNN (a), MNNNN (b), MNNMN (c), MMNMN (d), MMMMN (e) and MMMMM (f) (Nb-d or Mo-d refers to the d orbital of Nb or Mo atom at the interface, C-p refers to the p orbital of the C atom at the interface, Fe1 refers to the Fe atom adjacent to C or B at the interface, and Fe2 is adjacent to Nb or alloy atoms at the interface)

segregation of Mo on the Fe matrix side of the interface, and also slow down the segregation tendency towards Mo in NbC. B is more conducive to promoting the uniform distribution of Cr and Mo in the matrix.

Fig. 6c displays the Griffith fracture work when the replacement atom is located at position 1 and 3 after doping with B at the interface, that is, the interface separation work of the system after alloy elements are in the matrix and the interface, respectively. The figure uses the segregation energy of the corresponding alloy elements to color these 5 kinds of replacement atoms. It can be seen that when the replacement atom is in the Fe matrix, the interface separation work value is almost the same (about 5.65 J/m^2), indicating that the replacement atom has little effect on the interface separation work. When the replacement atom is located on the NbC side of the interface, except for Ni, the separation work of the system is generally higher than that when the replacement atom is located on the Fe matrix.

2.4 Electronic properties of alloy interface system

The replacement atoms have different effects on the interface bonding ability when they are at the interface. In order to more intuitively understand the atomic bonding between the replacement atom and its nearest atom, the charge density and the differential charge density of the adjacent atomic layer near the alloy phase interface were analyzed, as shown in Fig.7. In each alloy interface, Fe atoms or Nb atoms are replaced by specific alloy atoms. Therefore, different replacement atoms M (M=Si, Ni, Mn, Cr, Mo) may produce different bonding strengths.

The Griffith fracture work of the alloy interface in this

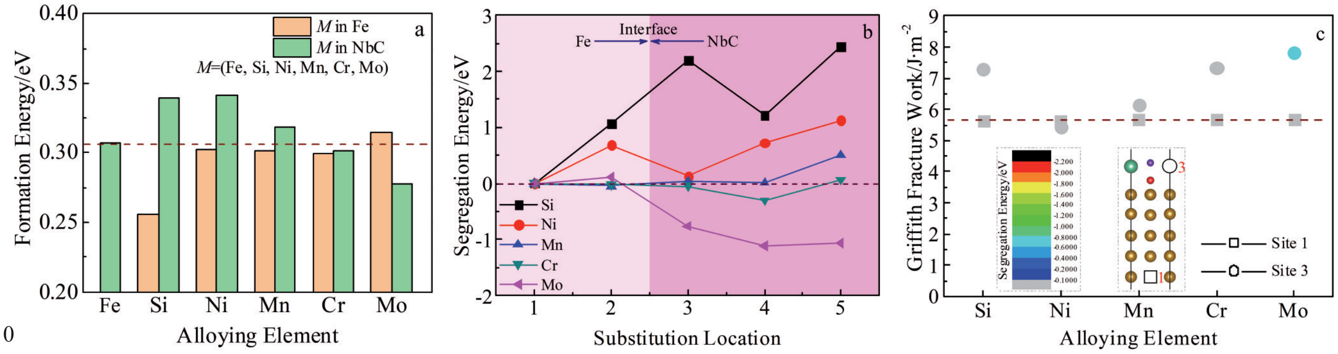

Fig.6 Formation energy of alloy element interface (position 1/5) after doping with B at the interface (a); segregation energy of alloy element interface (position 2/3/4/5) after doping with B at the interface (b); griffith fracture work of alloying interface after doping with B at the interface (position 1/3) (c)

study was calculated by dividing the interface into two surfaces. On the microscopic level, the cracking process of these phase interfaces is the destruction of Fe-C or M-C bonds. Therefore, the bonding strength of Fe-C or M-C bonds should make an important contribution to Griffith fracture work.

Taking different positions of Mo before and after B doping as an example, Fig.7a~7h show the charge density (1/2/3/5) of the Mo alloy interface before and after the interface doping with B. It can be found that the charge around the Fe atoms inside the Fe matrix is in a circular distribution, and there is no directional polarization distribution, indicating that the region presents certain ionic characteristics. Before the interface doping with B, it is found that the charge distribution around Fe (Mo) atoms at the interface has a certain directionality, and there is a large charge density in the middle area between Fe (Mo) atoms and the surrounding C atoms. Combining the electronegativity of Fe (Mo) and C, it can be considered that there is a polarized covalent (or ionic and covalent chemical bond) between Fe (Mo) and C, and the vertical axis on the edge of the graph represents the scale of the charge density value. After the interface is doped with B, when the replacement atom is on the Fe side, it is found that the polarized covalent (or ionic and covalent chemical bond) forms between Fe (Mo) and C at the interface. In addition, polarized covalent (or mixed chemical bond of ionic and covalent) also exists between B and C and between B and Fe (Mo). When the replacement atom is located on the NbC side, there is a large charge density of the middle area between B and the surrounding Fe and C. Combining the electronegativity of B, Fe and C, it can be considered that there is a polarized covalent (or a chemical bond of ionic and covalent mixing) between B and the surrounding Fe and C.

Fig. 7i~7p show the differential charge density of the Mo alloy interface (position 1/2/3/5) before and after doping with B. It can be seen that the charge transfer density at the interface before doping with B first increases and then decreases, and gradually stabilizes. This trend is consistent with the Griffith fracture work result of Mo alloy interface before interface is doped with B. The Mo atoms in the alloy interface (position 2) replace the Fe atoms at the interface. Due to the large amount of extra nuclear charge with Mo atoms, more charges are transferred to the opposite C atoms instead of Fe atoms corresponding to other interfaces so the C-Mo bond formed on the interface is slightly stronger than the C-Fe bond corresponding to other interfaces. Similarly, from the differential charge density at the Mo alloy interface doped with B, it can be seen that the charge transfer first decreases and then increases, and gradually stabilizes. This trend is consistent with the Griffith fracture work result of Mo alloy interface after interface is doped with B.

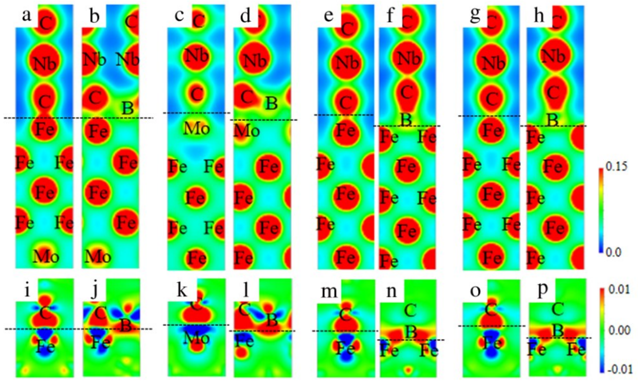

Fig.7 Charge density of the Mo alloy interface (position 1/2/3/5) before and after doping with B at the interface (a~h); differential charge density of the Mo alloy interface (position 1/2/3/5) before and after doping with B at the interface (i~p)

3 Conclusions

1) For the NbC/fcc-Fe interface, Cr and Mo can stably exist at the NbC/fcc-Fe interface and inside the NbC. In particular, Cr and Mo tend to segregate at the interface, and there is a tendency to further segregate to carbides. Si tends to be evenly distributed in the Fe matrix, and Ni and Mn tend to segregate at the NbC/fcc-Fe interface.

2) From the point of view on the (Nb, Mo)C composite carbide formed by dissolving Mo in NbC, the higher the solubility of Mo in NbC, the worse the stability of the system. That is, when the Mo/Nb content ratio reaches 2/3, the

(Nb,Mo)C composite carbide is more stable and has a greater binding energy, which should be related to the strong interaction between Mo, C and Fe.

3) B is more stable at the phase interface. The influence of B on the segregation behavior of alloy elements is analyzed. B suppresses the segregation tendency of Cr and Mo, especially on the interface, and improves the corrosion resistance of the material. Moreover, it is found that B can suppress the segregation tendency towards Ni and Mn, so that it can be uniformly distributed in the matrix Fe.

References

1 Zhang Shucai, Li Huabing, Jiang Zhouhua *et al. Corrosion Science*[J], 2020, 163: 108 295

2 Babu Arun K, Athreya C N, Mozumder Yahya H *et al. Metallurgical and Materials Transactions A*[J], 2020, 51: 3535

3 Li Xue, Zhang Ruofan, Wang Xiangyu *et al. Materials and Design*[J], 2020, 193: 108 750

4 Wang Jian, Cui Yishi, Bai Jingang *et al. Materials Letters*[J], 2019, 252: 60

5 Cui Yishi, Qurashi Muhammad Saqlain, Wang Jian *et al. Steel Research International*[J], 2019, 90: 1 900 041

6 Wang Chenchong, Shen Chunguang, Zhang Zhen *et al. Iron Steel Research International*[J], 2021, 28: 58

7 Zhao W X, Zhou D Q, Jiang S H *et al. Materials Science and Engineering A*[J], 2018, 738: 295

8 Zhang Zhengyan, Sun Xinjun, Wang Zhenqiang *et al. Materials Letters*[J], 2015, 159: 249

9 Wang Zhenqiang, Sun Xinjun, Yang Zhigang *et al. Materials Science and Engineering A*[J], 2013, 573: 84

10 Zhou Qingwen, Liu Jiangwen, Gao Yan. *Materials and Design* [J], 2019, 181: 108 056

11 Sanhueza J P, Montoya L F, Toledo E *et al. Steel Research International*[J], 2018, 89: 180 0215

12 Zhao Changchun, Xing Xiaolei, Guo Jing *et al. Applied Surface Science*[J], 2019, 494: 600

13 Zhou Yanyuan, Wang Zhenqiang, Zhao Jiaying *et al. Applied Physics A*[J], 2017, 123: 509

14 Hao Yansen, Li Jian, Li Xin *et al. Journal of Materials Processing Technology*[J], 2020, 275: 116 326

15 Perricone M J, Anderson T D, Robino C V *et al. Metallurgical and Materials Transactions A*[J], 2007, 38: 1976

16 Kresse G, Furthmüller J. *Physical Review B*[J],1996, 54: 11 169

17 Kresse G, Furthmüller J. *Computational Materials Science*[J], 1996, 6: 15

18 Perdew J P, Burke K, Ernzerhof M. *Physical Review Letters*[J], 1966, 77: 3865

19 Perdew J P, Chevary J A, Vosko S H *et al. Physical Review B*[J], 1992, 46: 6671

20 Blöchl P E. *Physical Review B*[J], 1994, 50: 17 953

21 Kresse G, Joubert D. *Physical Review B*[J], 1999, 59: 1758

22 Monkhorst H J, Pack J D. *Physical Review B*[J],1976, 13: 5188

23 Peng Mengmeng, Lai Wensheng. *Nuclear Instruments and Methods in Physics Research Section B: Beam Interactions with Materials and Atoms*[J], 2015, 352: 67

24 Liu S Y, Shang J X, Wang F H *et al. Journal of Physics: Condensed Matter*[J], 2009, 21: 225 005

25 Xie Y P, Zhao S J. *Computional Materials Science*[J], 2012, 63: 329

26 Wu Xuebang, You Yuwei, Kong Xiangshan. *Acta Materialia*[J], 2016, 120: 315

27 Fawaz Alnoman Mohammed Ahmed, Xue Hongtao, Tang Fuling. *Journal of Materials Science*[J], 2020, 55: 12 513

28 Adams J B, Hector Jr L G, Siegel D J *et al. Surface Interface Analysis*[J], 2001, 31: 619

29 Johnson D F, Carter E A. *Physical Chemistry A*[J], 2009, 113: 4367

30 Nai Qiliang, Zheng Wenjie, Song Zhigang *et al. Journal of Iron and Steel Research*[J], 2013, 25: 611 (in Chinese)

31 Williams T M, Stoneham A M, Harries D R. *Metal Science*[J], 2013, 10: 14

合金元素在NbC/fcc-Fe界面的偏析行为和硼的影响

杨　静[1]，张　翊[1]，董　楠[1]，李花兵[2]，韩培德[1]，姜周华[2]

(1. 太原理工大学 材料科学与工程学院，山西 太原 030024)

(2. 东北大学 冶金学院，辽宁 沈阳 110004)

摘　要：基于密度泛函理论（DFT）的第一性原理方法，研究了Si、Ni、Mn、Cr、Mo在NbC/fcc-Fe界面的偏析行为，以及B对合金元素界面偏析行为的影响。结果表明，Cr和Mo可以稳定存在于界面和NbC中；Mo更倾向于在界面和NbC中偏析；Ni和Mn在界面上有轻微的偏析倾向。另外，Mo容易偏析到NbC中形成复合碳化物。当Mo/Nb含量比小于2/3时，(Nb, Mo)C复合碳化物更稳定，结合能更大，这应该与Mo和C、Fe之间的强电子相互作用有关。当B掺杂到界面时，Mo和Cr向界面偏析的趋势被抑制。特别是B抑制了界面处Mo的偏析，从而提高了材料的耐蚀性。此外，B可使Ni、Mn趋于均匀分布在基体中。

关键词：合金元素；偏析能；NbC/fcc-Fe界面；硼；第一性原理

作者简介：杨　静，女，1997年生，硕士，太原理工大学材料科学与工程学院，山西 太原 030024，E-mail：1774365571@qq.com